PHILIPPINE ENGINEERING JOURNAL
PEJ 2021; Vol. 42, No. 1: 59-82

Stochastic Finite-Fault Modelling of Mw7.2 2013 Bohol Earthquake with Improvements via Low-Frequency Scaling Focusing on Time- and Frequency-domain Characteristics

Kristian M. Azul[1] and Mark Albert H. Zarco
[1] Geotechnical Engineering Group, Institute of Civil Engineering,
University of the Philippines Diliman, Quezon City 1101 Philippines

Abstract — *The deleterious effects of strong ground motions of earthquakes on structures are dependent on many factors which include the source, path, site, and as well as dynamic characteristics of the structure. Simulations of the strong motions corresponding to the October 15, 2013, Bohol earthquake were performed using a stochastic finite-fault modeling method while exploring the effect of low-frequency scaling. The simulated motion was then compared to the actual recorded ground motions using the peak ground acceleration, arias intensity, cumulative acceleration plots, Fourier amplitude spectrum, predominant frequencies, and goodness-of-fit values. Base simulations showed great similarity in overall envelope shape and PGA value. However, it was shown that simulations needed modification in the low-frequency range to better match the actual recorded motions. Improvement in the agreement between the simulated and recorded motions was achieved in both frequency-domain and time-domain characteristics, as well as goodness-of-fit values, after low-frequency scaling was applied. Although low-frequency scaling resulted in an accelerogram whose certain characteristics are closer to that of the recorded ground motions, it also resulted in an overestimated PGA value.*

Keywords — Earthquake Simulation, October 15 2013 Bohol Earthquake, Stochastic Finite Fault Model

I. INTRODUCTION

In the Philippines, seismic hazards pose a major threat to human life as well as human activities. This has necessitated the need to design structures and facilities that are resilient against prescribed levels of shaking described by a set of design ground motions. The Philippine Earthquake Model Atlas was recently launched by the Department of Science and Technology - Philippine Institute of Volcanology and Seismology (DOST - PHIVOLCS) and it contains peak ground acceleration (PGA) and spectral acceleration maps that were generated using Probabilistic Seismic Hazard Analysis [1].

The availability of modern seismographs and seismographic networks has made the recording and analysis of strong motion data promptly possible. Nevertheless, this development is relatively recent, particularly when compared with the time frames within which large-scale seismic events usually occur. To address this problem, various alternative approaches have been explored as a means for obtaining design ground motions. One such approach is the generation of artificial strong motion data. One of the methods used for creating ground motion prediction equations (GMPE) is the Stochastic Finite Fault Modelling (SFFM)

method, which considers the properties of the fault generating the strong motion [2] [3]. SFFM has been shown to be reliable in simulating motions where applications are mostly concerned with higher frequencies (1 – 10 Hz) but may have difficulty replicating the lower frequency range [2]. Consequently, EXSIM_V3 [2] [4] [5]- a program utilizing SFFM - has included scaling of low-frequency components to enable the resulting ground motion to be used in seismic hazard assessment. This is particularly useful in cases involving high-rise structures or subsurface configuration in which resonance occurs in the low-frequency ranges.

The PGA, Arias intensity, and Fourier amplitude spectrum (FAS) are some of the most widely used parameters for characterizing design ground motions. PGA and Arias intensity are referenced in the time domain, while the FAS is referenced in the frequency domain. Goodness-of-fit between two acceleration records may also be employed to quantify the closeness of the records when considering either their envelopes or phases.

SFFM with low-frequency scaling was used to obtain a synthetic accelerograph that aims to approximate the strong ground motions recorded from the October 15, 2013, M_w7.2 Bohol earthquake event. To generate the synthetic accelerograph, parameters characterizing the source, path, and site are used in the SFFM method. In cases where specific parameters are unknown, values proposed from past studies completed considering earthquake events in similar geologic settings are studied and used. A quantitative assessment of the simulated record's fit to the actual record is done by comparing the PGA, Arias intensity, FAS as well as goodness-of-fit values. Results of this study provide a basis for recommendations on the use of SFFM with low frequency scaling as an alternative method for obtaining design ground motions for seismic hazard assessment.

II. REVIEW OF RELATED LITERATURE

2.1 Time Domain Characteristics

Time-domain parameters are derived from data that is a function of time. The time-domain parameters studied are the peak ground acceleration (PGA), Arias Intensity (I_a), and cumulative acceleration plots (CAP).

The PGA is the absolute maximum acceleration that an accelerogram has [6]. PGA has various applications including liquefaction analysis, pseudo-static analysis as well as being a good index to hazard for building up to about 7 stories [7]. I_a, on the other hand, is a measure of the ground motion strength and is calculated as shown in equation 1 [6] [8].

$$I_a = \frac{\pi}{2g}\int_0^\infty [(a(t)]^2 dt \qquad \text{(Eq. 1)}$$

where I_a is the Arias intensity, $a(t)$ is the acceleration value at time t and g is the gravitational constant.

Cumulative Acceleration Plot or CAP is the sum of the absolute accelerogram values over time to show how the motion increases over time for the duration of the motion. This is

useful in comparing the evolution of motion over time between the simulation and recording. An example of an accelerogram and its CAP is shown in figure 1.

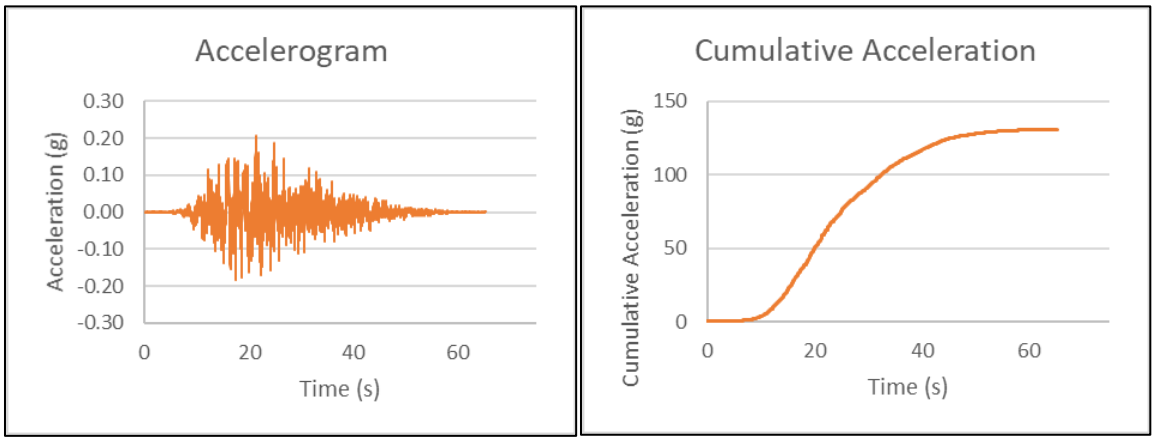

Figure 1. An accelerogram (left) and its cumulative acceleration plot (right)

2.2 Frequency Domain Characteristics

Frequency domain parameters are derived after time-domain data (i.e. accelerogram) is transformed to be shown as a function of frequency. One can rewrite a periodic function as the sum of simple harmonic terms via the Fourier series as shown in equation 2 [6].

$$x(t) = c_0 + \sum_{n=1}^{\infty} c_n \sin(\omega_n t + \phi_n) \quad \text{(Eq. 2)}$$

where c_n, ϕ_n, and ω_n are the amplitude, phase angles, and frequencies, respectively, for the *n*th harmonic [6]. The Fourier amplitude spectrum (FAS) is the plot of the amplitude versus the frequency and shows which frequencies have the most contribution in the motion [6]. The frequency value where the maximum frequency content is located is called the predominant frequency [6].

2.3 Stochastic Finite-Fault Modelling Method and EXSIM_V3 Program

Stochastic Finite-Fault Modeling (SFFM) is widely used to predict ground motions based on the characteristics of the source, path, and site effects [4] [2]. Crane and Motazedian (2013) have listed several papers that used SFFM in predicting moderate to large earthquakes while Atkinson and Boore (2006) have used it in studies related to ground motion prediction equations (GMPEs) [2] [3]. SFFM consists of 2 concepts used together – the stochastic method and finite fault modeling. Stochastic methods combine the ground motion arbitrariness with earthquake characteristics so that these characteristics are reflected and possible motions are simulated [4] [2]. Stochastic methods must follow a strict order of processes to ensure correct results [4] [2] [9]. This procedure is discussed in more detail in the manual of EXSIM_V3 – a program that utilizes SFFM [4]. Finite fault modeling is employed with the stochastic method but allows the subdivision of the fault into sub-faults (which are treated as point sources) and the sub-faults' contributions are summed together with the computed time delay, which results to the larger, desired ground motion [4] [2] [3].

SFFM has been useful in replicating ground motions in the 1-10 Hz frequency range, but not as much likeness can be seen in the lower frequencies of its results [2]. Low-frequency (<1 Hz) is an important part of civil engineering works, especially in high-rise buildings as these buildings tend to have a higher natural period (lower natural frequency).

EXSIM_V3 is a program that is based on SFFM and is used in this study [4] [2]. It was chosen as the program to be used (among various EXSIM variants available) as this version has the optional function of low-frequency scaling. The low-frequency scaling options in EXSIM_V3 allow the modification of the earthquake simulation's low-frequency range so that it may approximate the low-frequency content of the actual record [4] [2]. More details on the implementation of the low-frequency scaling options are found in the EXSIM_V3 manual and paper by Crane and Motazedian (2013) [4] [2]. The concept of dynamic corner frequency, developed to address the dependency of previous finite-fault programs to sub-fault size, is implemented in the program [4] [10].

2.4 H/V Method

The H/V technique is a technique used to get an approximation of the site amplification using surface records from a station if there is no surface to bedrock data available. The H/V ratio can be used as a rough approximation of the site amplification as it has a resemblance to the transfer function [11]. The original paper of Nakamura (1989) had pointed out that the earthquakes' H/V spectral ratio is quite similar to the amplification spectra [11] [12]. It was also confirmed that the microtremors' and earthquake motions' H/V spectral ratios are similar and mostly similar to the amplification spectrum as well [13] [12]. The H/V method will be utilized in this study to approximate site effects needed for the simulation.

III. METHODOLOGY

3.1 Simulation Process

Earthquake simulations of the October 15, 2013, M_w7.2 Bohol earthquake are done using the stochastic finite-fault modeling method employed by the EXSIM_V3 along with its low-frequency scaling option. The record used from the earthquake is from the TBPS recording station. Simulations without any low-frequency scaling are done and compared to the actual earthquake recording from the said site using the earthquake characteristics discussed prior. After analysis, amplification on certain frequency ranges is applied to achieve a better fit in the frequency content between the simulation and actual record.

The data needed to model the earthquake can be categorized into three – source, path, and local site input [4]. Source inputs are related to the fault itself (dimensions, the energy released, etc.); Path inputs modify the motion as it travels through the earth (ex. shear wave velocity, attenuation factors, etc.); and lastly, local site input takes into account the changes due to the site itself (local motion amplification based on the subsurface, among others) [4].

3.2 October 15, 2013, M_w7.2 Bohol Earthquake Input Parameters

A devastating earthquake struck Bohol, Philippines last October 15, 2013. According to the SWIFT Centroid Moment Tensor Solution from DOST - PHIVOLCS, it had a Moment

Magnitude of 7.2 [14]. The estimated depth of the earthquake event is 12 km [15] [16]. The earthquake was generated by an unmapped fault [17]. At the time of the research, there is no official published map of the fault. The fault was mapped out based on the various maps and personal communication (M. L. Bautista, Personal Communication, January 11, 2016) [17] [18] [19]. From the magnitude of the earthquake, the width of the fault is computed as 15 km using the relations from Wells and Coppersmith (1994) [20]. The dip angle used is 46º [21] [14]. An idealized fault model was made, and the depth of the fault was determined to be 1.35 km to fit the hypocenter location. The idealized fault line along with the epicenter and TBPS recording station is shown in Figure 2.

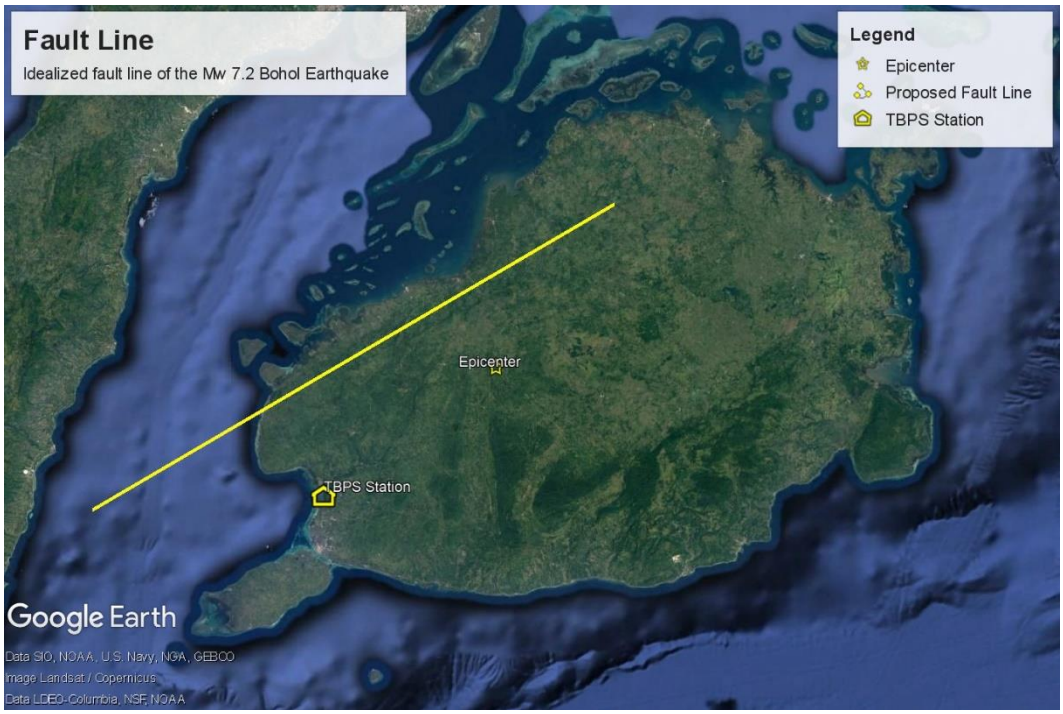

Figure 2. Map of Bohol showing the Epicenter, idealized fault line, and TBPS recording station.

Map data: Google Earth; Google; Data SIO, NOAA, U.S. Navy, NGA, GEBCO; Image Landsat/Copernicus; Data LDEO-Columbia, NSF, NOAA [22] [23]

For the crustal amplification values, the bedrock underlying the site is assumed to be soil profile type A based on NSCP 2015 soil profile types [24]. This was assumed based on the information that Bohol is mostly underlain by Maribojoc Limestone on the western part which also covers the epicenter and TBPS station [25] [26]. The crustal amplification files for hard rock sites were used for this simulation [3] [27].

H/V ratio utilizes the record at the TBPS station to get the site amplification. A 40-second segment of the earthquake record was used for this method [28]. Figure 3 shows the earthquake records from DOST-PHIVOLCS with the used segment highlighted [29]. The earthquake record is shown in blue, and the 40-second segment used is shown in orange. The resulting site amplification spectrum used for the simulation is in figure 4.

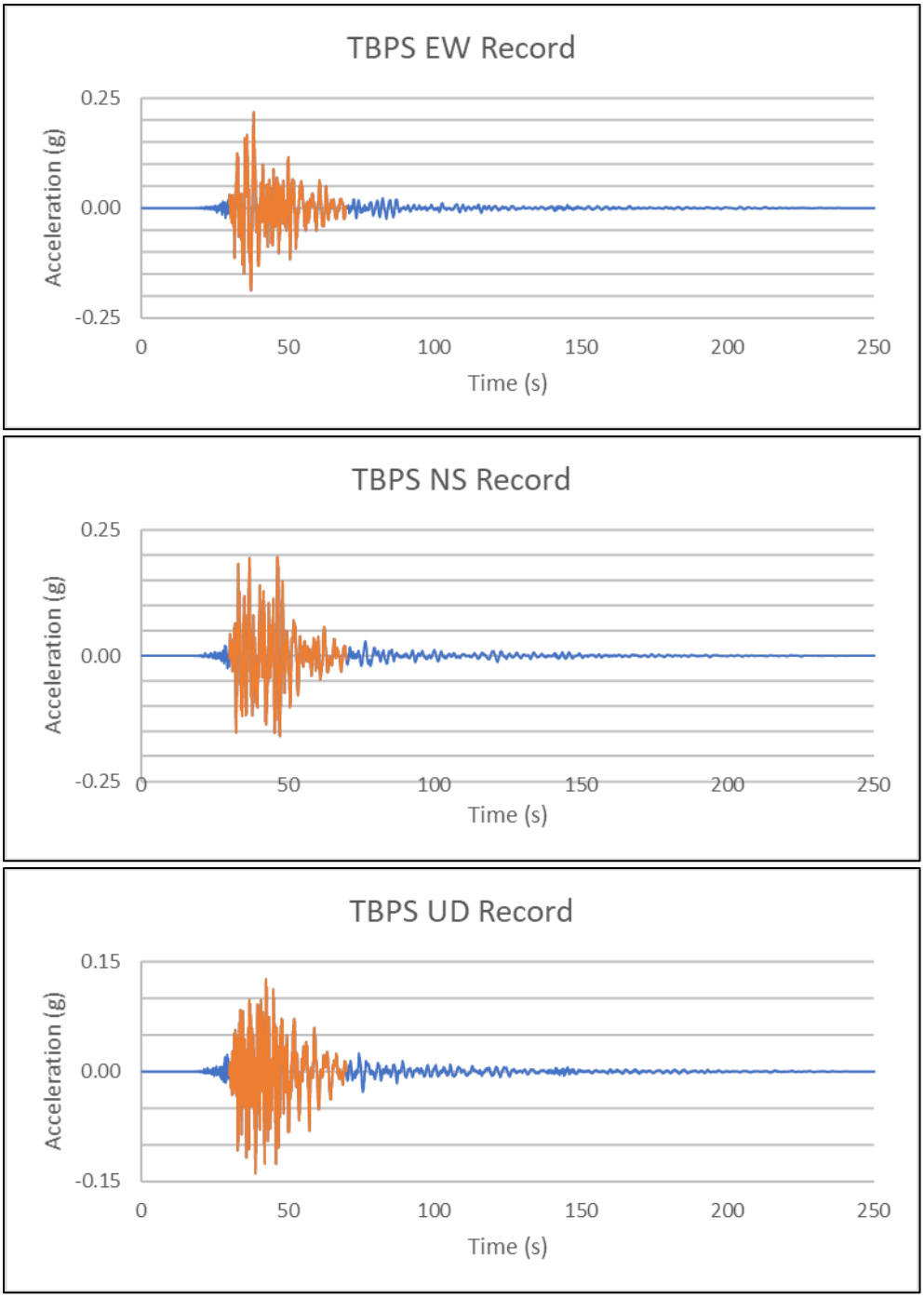

Figure 3. EW (top), NS (middle), and UD (bottom) record for the whole earthquake event (blue and orange) with extracted 40-second segment (orange)

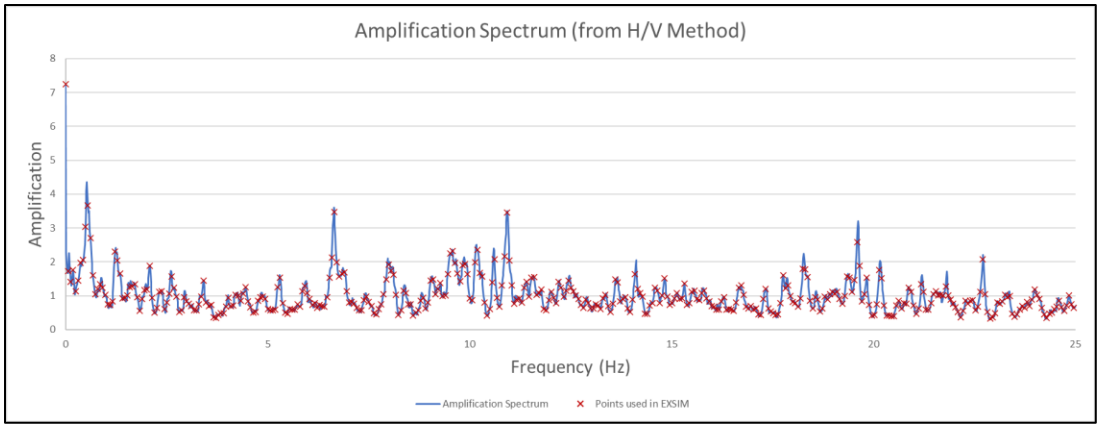

Figure 4. Site amplification graph showing the points used as input (marked by red asterisks) for the EXSIM_V3 program

Some parameters do not have values that are specific to the event or the site. For this, the values used are taken from literature from countries like Taiwan and Japan, which are accepted as countries with similar earthquake-related characteristics as the Philippines.

The parameter kappa, (κ) is used to model the property of earth that filters high frequencies [4]. This parameter is assumed to be 0.03 for simulations performed in this study based on previous simulations for Taipei, Taiwan [30] and Tohoku, Japan earthquake [31] [32].

The shear wave velocity and density used are 3.6 km/s and 2.8 g/cm^3, respectively, patterned after studies in Taiwan [33] and Tohoku, Japan earthquake [31] [34]. The ratio of rupture velocity to shear wave velocity was taken to be 0.8, the average value of the usual range of 0.7 – 0.9 [35]. The geometrical spreading used is R^{-1}, where R is the distance from the source, patterned after a study of the Tohoku, Japan earthquake [31] [36]. It was noted earlier that Bohol has limestone underneath. Due to this, the quality factor function used is based on the paper of Kanao and Ito (1992) that determines this quantity for the North area of the Philippines including Baguio (that also sits on limestone) [37]. The quality factor function is $Q = 68f^{1.06}$ [37] and Qmin is assumed to be 0. Although this is coda wave attenuation, this is the closest attenuation study that can be used given the similarities in the sites and lack of available proper attenuation study for shear waves in the area. The duration function form employed in EXSIM_V3 is of the generic trilinear form [4]. However, the duration function, D(x), in this study is simplified to a linear function in terms of the source-to-site distance, x, of the form:

$$D(x) = m\,x + b$$

where b is the minimum duration value, and m is the rate of increase in the duration with the source-to-site distance. The distance-dependent property of duration is patterned closely after studies from the Chichi earthquake [38] and Tohoku, Japan earthquake [31] [39]. The minimum duration value is adjusted until the simulation record (test case 1; test cases will be

discussed a few paragraphs below) is similar to the actual records based on visual comparison of the shape or envelope of the accelerogram. The duration function is shown in equation 3.

$$D = 30 + 0.1R \quad \text{(Eq. 3)}$$

where *D* is the total duration of the motion and *R* is the distance between source and site.

Stress drop is one of the parameters that control the levels of the spectrum in ranges usually greater than 1 Hz [40]. Initially, trial-and-error was employed until test case 1 simulation has a PGA value very close to the actual recorded motions' PGA values. The stress drop used is 100 bars. This value is the same value used in a simulation of the West Valley Fault (WVF) earthquake by Pulido et.al. [41]. WVF has a comparable fault size and magnitude to the Bohol event [42].

The low-frequency scaling module will be used when the initial outputs are not sufficient to approximate the frequency content of the actual records. EXSIM_V3 has three low-frequency scaling options, two of which allow scaling or modification of the frequency content based on additional scaling parameters defined by the user [4]. The first low-frequency scaling option is the usage of a Filter Function by Boore (2009) that uses the number of sub-faults, among others, as an input to address the problematic sub-fault spectra summation for certain frequency ranges [4] [2] [43]. This low-frequency scaling option does not take in a value that can be adjusted by the user to directly affect the amount of scaling. The low-frequency scaling option used to modify the low-frequency range is the Empirical Function where a scaling value is applied over a frequency range defined by the user [4] [2]. This allows the scaling of a specific frequency range of motion and a scaling value that can be easily adjusted by the user. There are 4 test cases (TC) of simulations done with each targeting a specific characteristic of the recorded earthquake event. TC 1 uses the Filter Function. TC 2 uses the Empirical Function low frequency scaling method but with a multiplier of 1 – a TC that uses a low-frequency scaling method without any actual scaling done. TC 2 serves as our guide in amplifying the frequency content for the next TCs. TC 1 and TC 2 can be considered as "base cases" since TC 1 aims to apply correction only due to the subdivision of the fault into sub-faults and TC 2 does not apply any correction at all. TCs 3 and 4 aim to approximate the frequency content (especially in the low frequencies) of the EW and NS actual records, respectively.

IV. RESULT AND DISCUSSION

The motion recorded by the TBPS station is shown below. The original record is more than 200 seconds long, as sourced from DOST-PHIVOLCS [29]. An initial bracketed segment is identified by identifying the first and last exceedance of 0.001g to be used as the initial comparison segment for simulation. A further shortened version of the bracketed segment is shown in Figure 5.

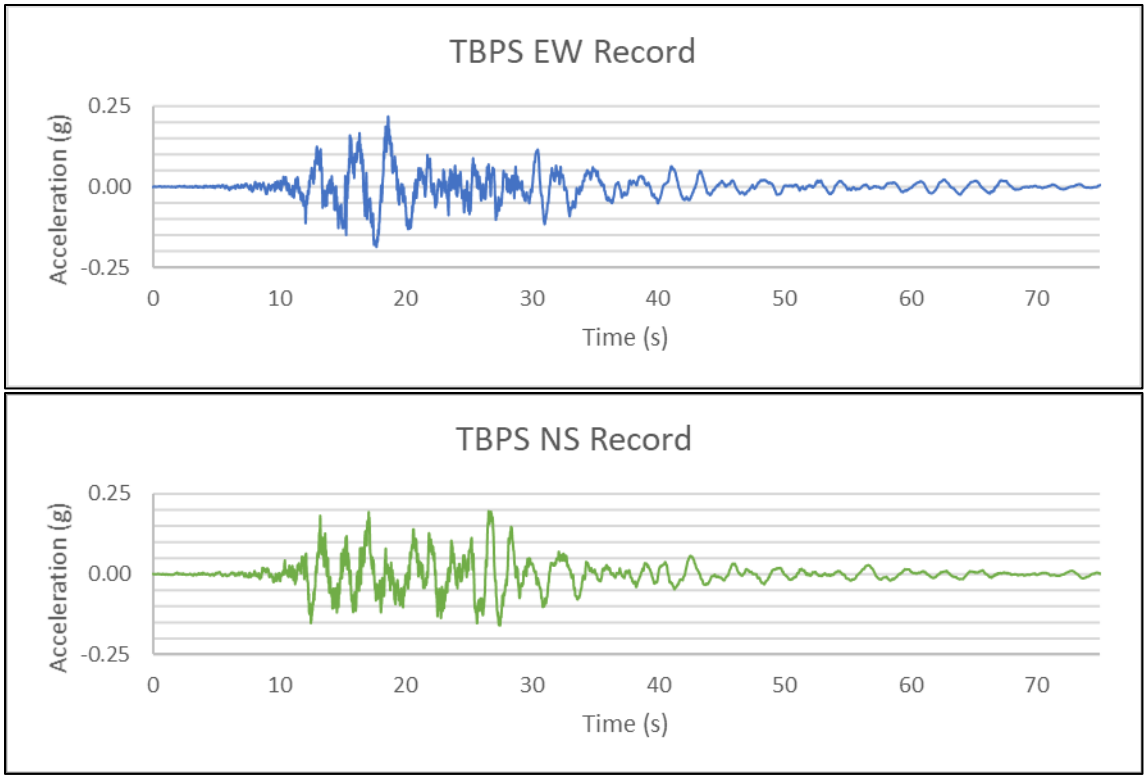

Figure 5. TBPS accelerogram record: TBPS EW recording (top) and TBPS NS recording (bottom)

4.1 Base Test Cases (1 and 2)

TC 1 is based on the input with corrections based on the fault's subdivision. Figure 6 shows the comparison of various plots of TC 1 simulation vs TBPS records (EW and NS).

With the stress drop used, the peak ground acceleration (PGA) of the simulation is 0.21g – midway between the PGA of EW and NS records that is 0.22g and 0.20g, respectively.

The shape was easily approximated for this earthquake event. This is due to the enveloping function used by EXSIM_V3 being very close to the shape of the envelope of the TBPS recording. While the shape of the TBPS recording is similar to the envelope function used in the program, one parameter that can greatly affect the shape similarity of the TBPS recording and the simulation is the duration function of the earthquake simulation (aside from the stress drop). The duration function affects how long the simulated motion will be and the stress drop affects how high the peak will be. Together, they can affect the overall shape of the recording.

The CAPs shown in figure 6 indicate that the simulation approximates the increase of motion over time of the TBPS recordings. However, the simulation also flattens out sooner than the TBPS recording in this respect.

Despite what seems like very good agreement in the accelerogram of the simulation and TBPS recording, it can be shown that there is a significant difference in the simulation and recording when the frequency content is analyzed via the FAS. The FAS in figure 6 shows that

there is very little frequency content in the low-frequency range of the simulation as compared to the TBPS recording. It can also be seen, although not as pronounced, that the frequency content of the simulation in the high-frequency range is higher than those of the TBPS recordings.

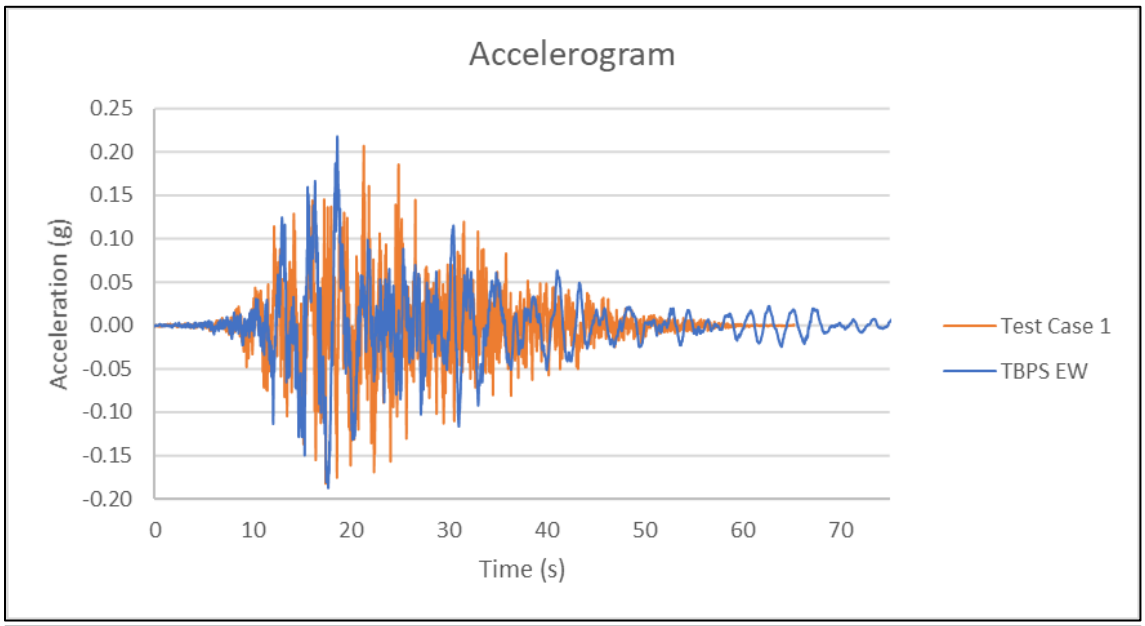

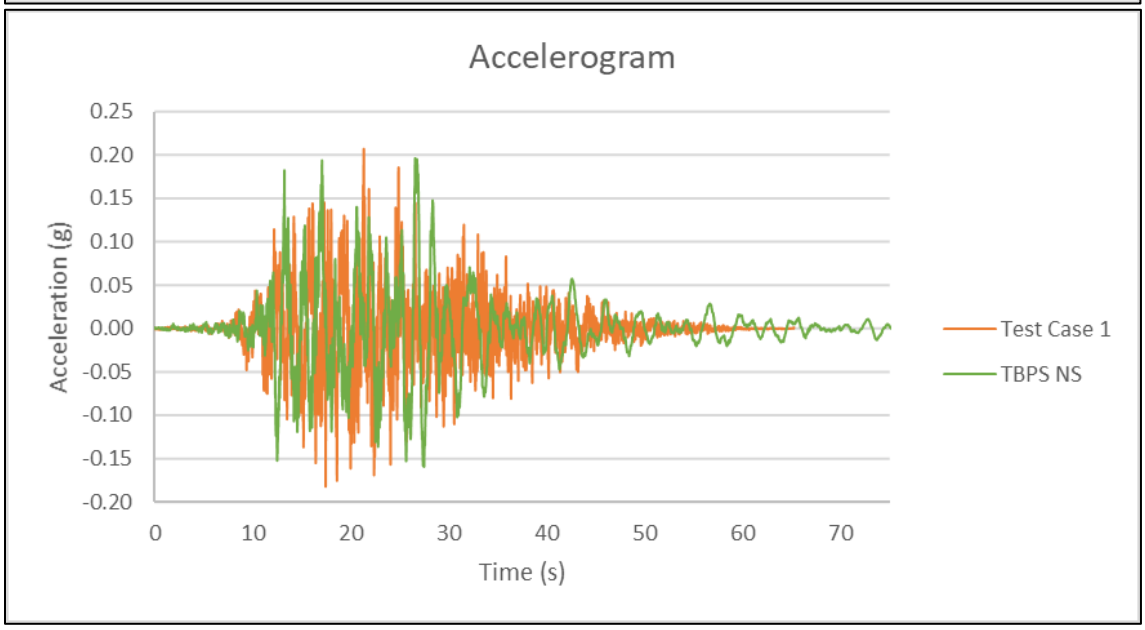

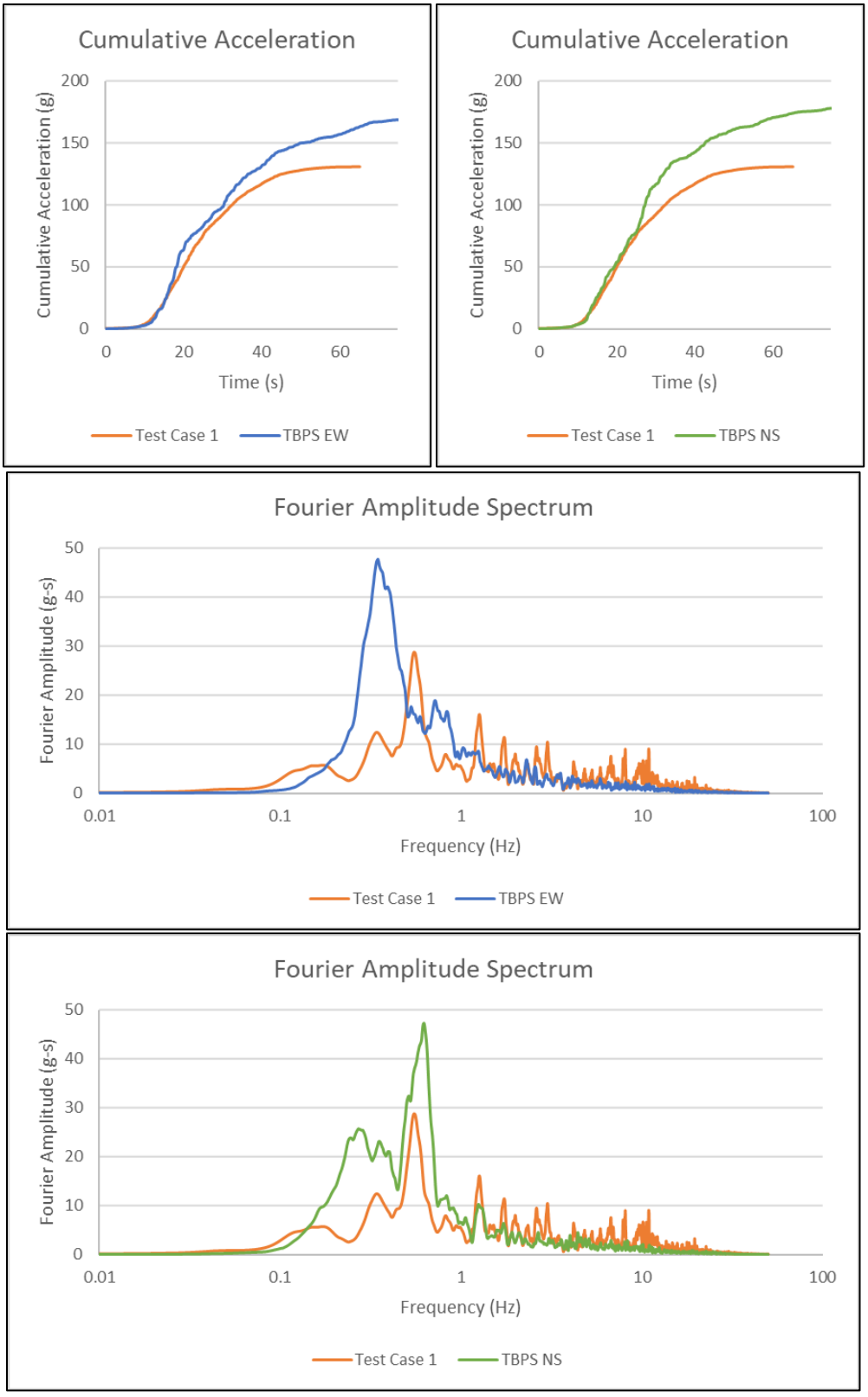

Figure 6: Comparison of TC 1 and TBPS records:
Accelerogram (1st row: TC 1 vs EW ; 2nd row: TC 1 vs NS)
CAP (3rd row left: TC 1 vs EW ; 3rd row right: TC 1 vs NS)
FAS (4th row: TC 1 vs EW ; 5th row: TC 1 vs NS)

TC 2 is almost identical to TC 1. The main difference is that due to the correction done in TC 1, its low-frequency range content is slightly greater than that of TC 2 but almost indistinguishable. A comparison of the accelerogram, CAP, and FAS of TC 1 and 2 is shown in figure 7.

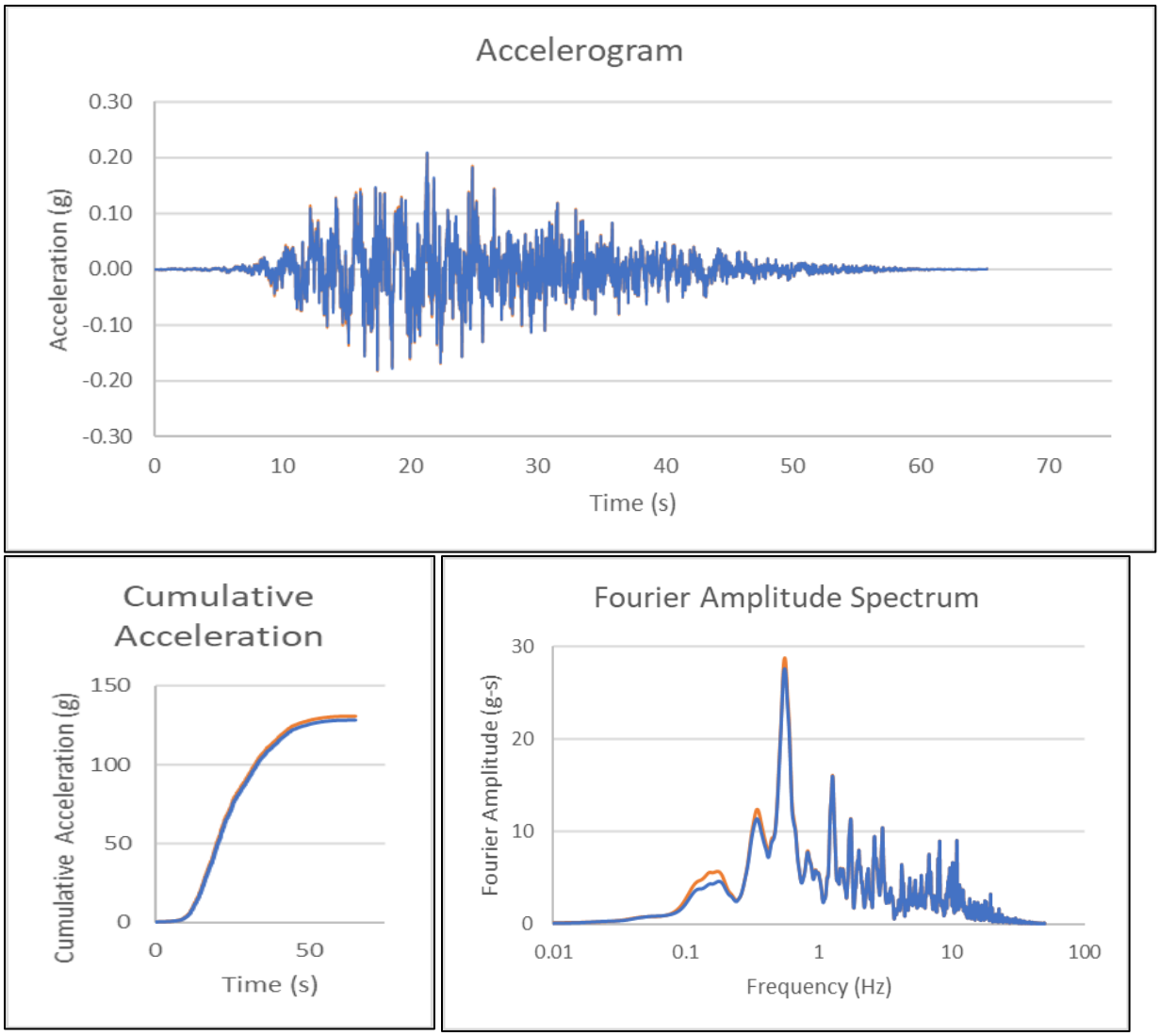

Figure 7. TC 1 (orange line) VS TC 2 (blue line) earthquake characteristics comparison: Accelerogram (top) ; CAP (bottom left) ; FAS (bottom right)

4.2 Test Case 3

TC 3 aims to approximate the frequency content of the TBPS EW recording using the low-frequency scaling option of the program. We use TC 2 as a baseline and identify the range of low frequencies that are significantly less in our simulation compared to the TBPS EW recording. The range and amplification factors are refined to get a better fit. It was found that an amplification factor of 4.25 and an amplification range of 0.24 Hz to 0.48 Hz produced the best fit among the trials. Figure 8 shows the comparison between TC 3 and TBPS EW records.

Considering the FAS of our TC 3 simulation, there is a significantly better agreement with the TBPS EW recording's FAS, especially in the low-frequency range. The peak of the FAS is approximated well while there is still lacking frequency content around the 1 Hz value. Furthermore, the overestimation in the higher frequencies remains.

The accelerogram and the CAP are shown in figure 8. It is seen that due to the amplified low-frequency content, the accelerogram appears to have a more pronounced separation between peaks compared to the simulations prior and this is a better approximation of the actual record. It can also be seen that the CAP shows most of the intensity of the original. It is lacking at the end due to the record being shorter but what we lack are the trailing weak motions only.

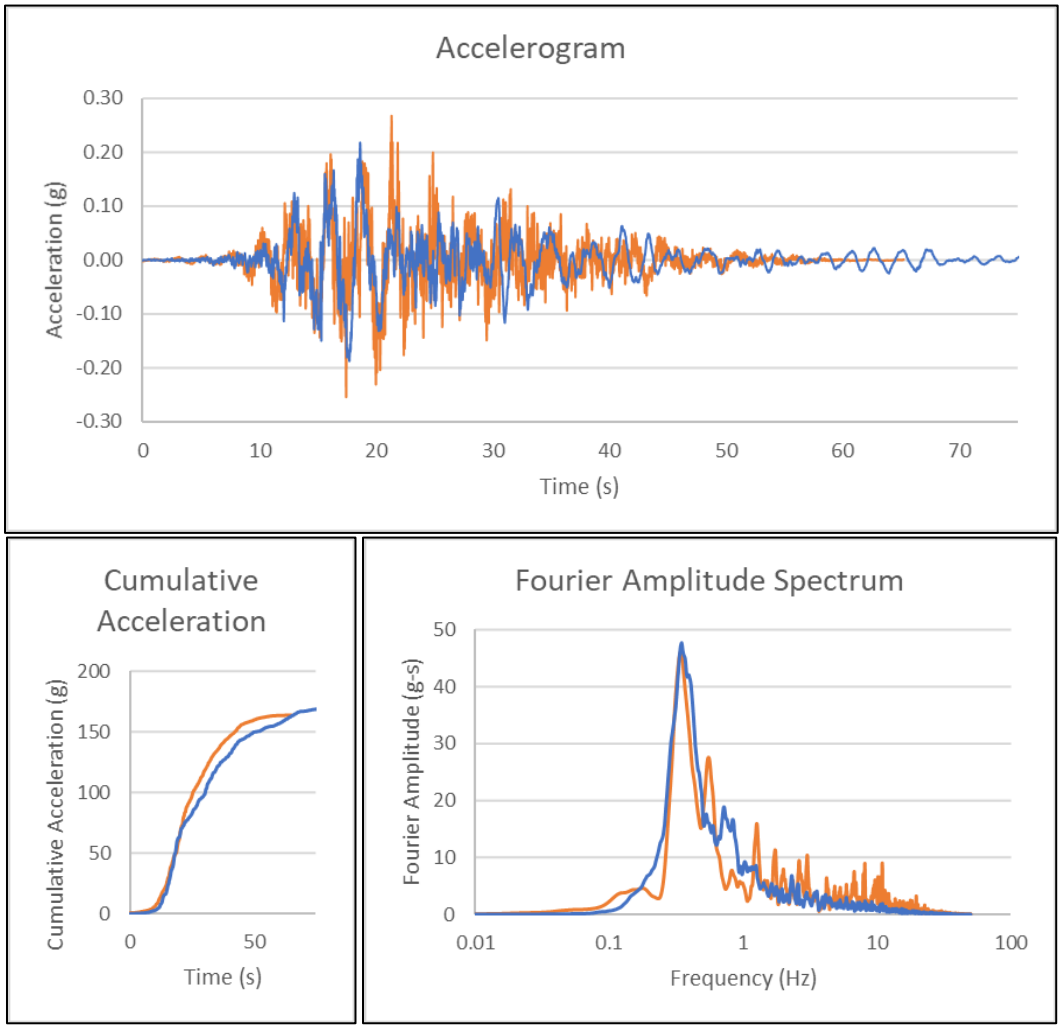

Figure 8. Comparison of TC 3's (orange line) and TBPS EW record's (blue line) earthquake characteristics: Accelerogram (top) ; CAP (bottom left) ; FAS (bottom right)

4.3 Test Case 4

TC 4 approximates the frequency content of the TBPS NS recording using the amplification module of the program. After refining the amplification value and range, the best simulation required an amplification value of 2.00 and an amplification range of 0.44 Hz to 0.80 Hz. Figure 9 shows the comparison between TC 4 and TBPS NS records. As seen, the frequency range 0.10 Hz to 0.40 Hz was not included in the amplified range and has great discrepancies. This is because including this range in the amplified range will result in frequency content at that range over-estimating that of the actual record's.

It can be seen in the accelerogram that increasing the low-frequency content of the simulation resulted in a motion with seemingly greater separation between peaks, similar to what happened in TC 3 simulation. This gives us a simulation that is closer to the TBPS NS recording of acceleration. The CAP likewise supports the similarity of the accelerogram. As seen, the CAPs have very close slope values, with the simulation only falling off once the motion has died down.

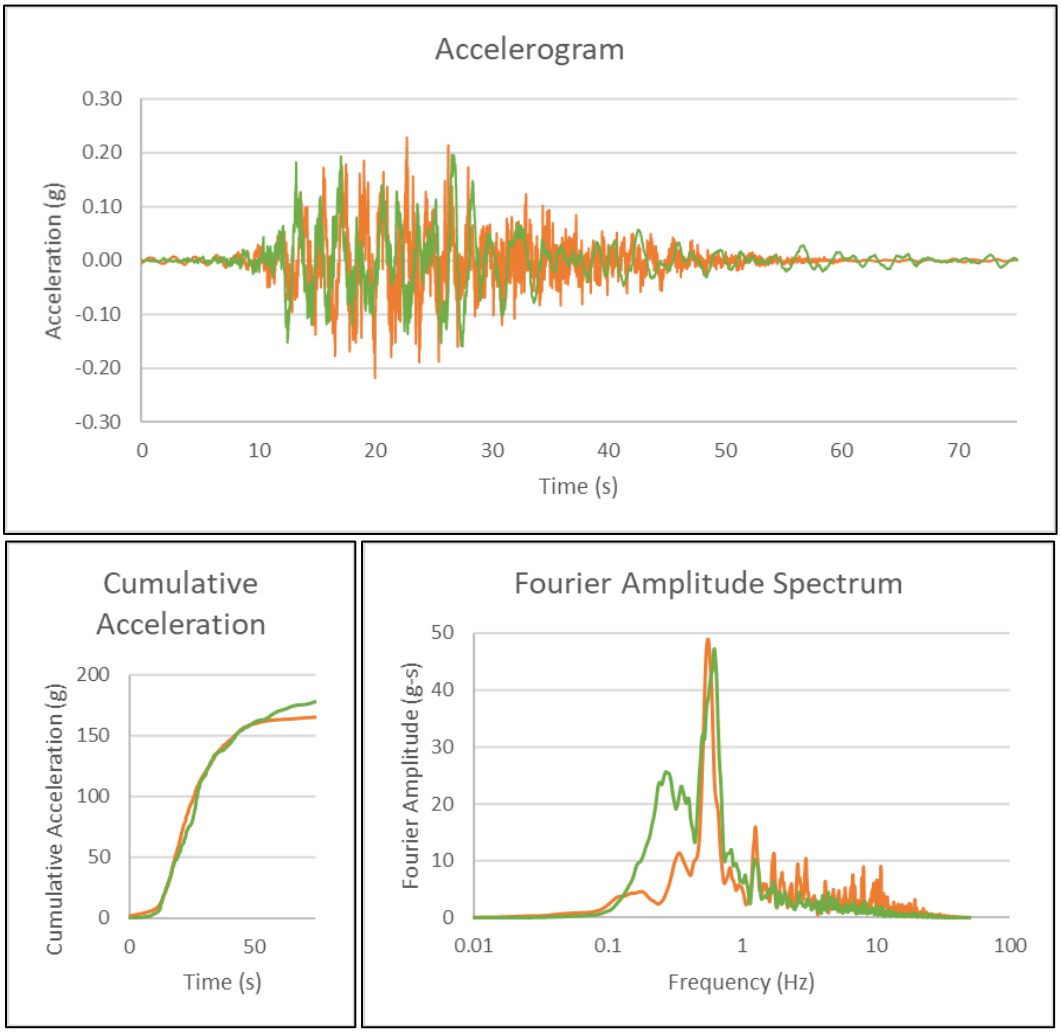

Figure 9. Comparison of TC 4's (orange line) and TBPS NS record's (green line) earthquake characteristics: Accelerogram (top) ; CAP (bottom left) ; FAS (bottom right)

4.4 Test Comparisons

Normalized residuals of certain earthquake characteristics are compared in the succeeding sections. These were normalized by the same earthquake characteristics computed from both the EW and NS records. Equation 4 shows how this is applied on an earthquake characteristic, X:

$$X\%_{Normalized\ Residual} = 100 * \frac{|X_{test\ case} - X_{actual}|}{X_{actual}} \qquad \text{(equation 4)}$$

Where $X\%_{\text{Normalized Residual}}$ is the normalized residual of X in %, and the subscript refers to the record whether being a TC record or actual record. The actual record can be EW or NS.

Table 1 shows a summary of the PGA for each TC and actual record along with the normalized residual (as compared to EW and NS recording PGA). As seen, the minimum residual is found in TC 2 (versus TBPS EW recording) and TC 1 (versus TBPS NS recording). And as shown, our attempts at approximating the frequency content of our actual recordings gave a higher PGA than our base cases (1 and 2).

Table 1. PGA Normalized Residual Values

Test Cases	PGA (g)	Residual in % (Normalized by EW Actual Value = 0.22g)	Residual in % (Normalized by NS Actual Value = 0.20g)
TC 1	0.21	4.99	5.51
TC 2	0.21	4.03	6.58
TC 3	0.27	22.83	36.40
TC 4	0.23	4.83	16.42

Table 2 shows a similar table as table 1 but for the Arias intensity. While the comparison between PGA seemingly favors the base TCs, the Arias intensity shows very different results. As shown, the TCs targeting the FAS of a specific direction of the record showed significantly less difference in the Arias intensity. It must be noted that the minimum arias intensity residual is not observed between the TC targeting the FAS of a specific direction of the record (TC 3 targets EW's FAS and TC 4 targets NS's FAS). The TCs targeting the FAS of a specific direction of the record still show significant improvement from the base TCs. Arias intensity residual of TC 3 (compared to EW record) being ~40% of the base TCs; and Arias intensity residual of TC 4 (compared to NS record) being ~15% of the base TCs.

Table 2. Arias Intensity Normalized Residual Values

Arias Intensity (m/s)			
Test Cases	Value	Residual in % (Normalized by EW Actual Value = 1.66)	Residual in % (Normalized by NS Actual Value = 1.88)
TC 1	1.18	29.32	37.46
TC 2	1.14	31.65	39.52
TC 3	1.87	12.12	0.78
TC 4	1.77	6.27	5.96

Another part of the FAS that can be used to compare the simulation to the actual recording is the predominant frequency – the frequency where the peak FAS value is located. Determining the predominant frequency helps determine where there may be significant resonance effects on the frequency range. However, this may fail to capture other frequency values where there is significant frequency content as well since the predominant frequency is of a single value. As seen in the previous figures, the predominant frequency of TCs 1 and 2 is quite close to the TBPS NS record. TCs 3 and 4 significantly improve the agreement between the predominant frequencies between the simulation and targeted recording while also bringing the frequency content distribution much closer as well.

Table 3 below shows two criteria in comparing the frequency content (FAS) of the TCs to the actual records – namely, the Root Mean Square Error (RMSE) and Mean Absolute Error (MAE). The RMSE and MAE show minimum values for the TCs targeting the FAS of a specific direction of the record while all the other TCs have RMSE and MAE values that are roughly close. For the EW recording, the base TCs have RMSE and MAE of ~2.37 and 0.84, respectively, but TC 3 has 1.58 and 0.75 - an evident improvement over the base TCs. The same can be observed for NS recording where RMSE and MAE improve from ~2.16 and ~0.83 to 1.86 and 0.79, respectively.

Table 3. FAS RMSE and MAE Values

Test Cases	RMSE		MAE	
	EW	NS	EW	NS
TC 1	2.35	2.14	0.84	0.82
TC 2	2.38	2.18	0.84	0.83
TC 3	1.58	2.20	0.75	0.83
TC 4	2.63	1.86	0.88	0.79

Kristekova et al. (2009) defined a goodness-of-fit (GOF) value (based on time-frequency misfit values) that is used to quantify the "closeness" of 2 accelerograms (with one used as a reference) [44] [45]. GOF values range from 0 to 10 with higher values meaning greater closeness of the compared records [44]. As records may differ in either amplitudes/envelopes or phase (or both), the GOF concept was applied to both envelope and phase [44] [45]. The

envelope GOF and phase GOF values are shown in table 4 for the different TCs as compared to TBPS EW and NS records, along with the interpretation of values based on Anderson (2004) and as shown in Kristekova et al. (2009) [46] [44]. The program package discussed in Kristekova et al (2009) can be found on the Nuquake website [44] [47]. The envelope GOF values are abbreviated as EG and the phase GOF values are abbreviated as PG in the table and discussion that follows.

Table 4. GOF values for each TC with TBPS record as the reference

Test Cases	EW as reference motion				NS as reference motion			
	EG		PG		EG		PG	
1	4.69	Fair	6.01	Good	4.90	Fair	3.88	Poor
2	4.65	Fair	5.99	Fair	4.87	Fair	3.91	Poor
3	5.94	Fair	6.23	Good	4.57	Fair	3.90	Poor
4	4.28	Fair	2.30	Poor	5.21	Fair	5.04	Fair

The GOF values show that TC 3 and TC 4 are the most similar records to the TBPS EW and NS records, respectively. When EW record is used as the reference, although all TCs fall within the same "fair" category based on EG, TC 3's EG is bordering towards "good" fit (6 being the boundary between fair and good categories [46]). PG on the other hand is quite similar for most TCs, except TC 4 where the PG dropped drastically. When the NS record was used as a reference, TC 4 had a slightly better EG value than the rest of the TCs. PG for the TCs 1 to 3 are almost equal and a much better "fit" is observed for TC 4. It must be noted though that the EG and PG values more relevant when referenced against EW record would be that of TC 3's as it was the TC targeting the FAS of EW record (and TC 4 would be more relevant when NS record is used as reference). Ultimately, the fits, even with low-frequency scaling applied were only good at best. This provides another view of how approximating FAS may not be enough to be able to fully capture an earthquake event. Although an argument can be made as to what "similarity" you ultimately need from your simulations – will it be earthquake characteristics like PGA, predominant frequency, or will you put more weight in certain responses from the simulation (acceleration, velocity, or displacement)?

V. CONCLUSION AND RECOMMENDATION

Simulations without low-frequency scaling, show good agreement for PGA values only. Even without low-frequency scaling, the agreement between the PGA of the simulation and the actual record can be achieved by adjusting the value of the stress drop. Due to the scarcity of literature on the appropriate range of stress drop values to use for a given source, it is recommended that the stress drop value be adjusted until the acceleration values (including the PGA) of the simulation are about the same as those of the original records'. An area for further research is the development of a rational procedure or empirical relationship to estimate stress drop value based on other earthquake characteristics. In the absence of such a rational procedure or empirical relationship, the authors recommend adopting stress drop values used in previous simulations performed on similar-sized events with similar source characteristics. This is most useful in analyses where PGA is the sole earthquake-related input, and no transient

record is needed. One of the applications is in the computation of the cyclic stress ratio pertinent to liquefaction susceptibility analysis [48] [49]. These also provide acceptable input for pseudo-static analyses where PGA is used to compute inertial forces. Base simulations (TC 1 and TC 2) will also be very useful in the creation of various hazard correlations for structures up to seven stories as PGA is a good index for such studies [7]. In such cases, using SFFM without low-frequency scaling can be used as an alternative to obtaining PGA using empirical attenuation relationships.

Simulations with low-frequency scaling show improved Arias intensity values and CAP, as well as frequency content approximation. The improved frequency content in low-frequency ranges is most useful in analyses considering structures with natural frequency less than 1 Hz as this will generally show higher responses in the low-frequency ranges in the response spectrum from the earthquake. This means that if a response spectrum is to be used in a study or design, low-frequency scaling becomes more pertinent if you are studying structures in the low-frequency range (<1 Hz). Overall, the application of low-frequency scaling brings more advantages for processes that require transient motion records like ground response analysis. From the discussion, there is a substantial improvement for the test cases with low-frequency scaling for the Arias Intensity, CAP, and FAS. The better approximation of Arias intensity bodes well for our simulation as this reflects the shaking in a site. The FAS is a very important property as well to be approximated well as this can highly affect the response spectrum of the earthquake record and ground response analysis results. While the application of low-frequency scaling increases the PGA of predicted ground motion, the authors are of the opinion that the increase will likely not have a significant impact on the design based on the increase in PGA observed in this study. If earthquake records with a prescribed PGA value are needed, such as in the case of Ground Response Analysis, scaling of the earthquake record is usually employed. Alternatively, one can explore adjusting other input parameters– preferably, without significantly affecting the other earthquake characteristics. The GOF values (EG and PG) improvement may not always be substantial, but it still shows that simulations with low-frequency scaling are generally better than the ones without (when targeting a specific record's frequency content). Furthermore, the authors believe that an earthquake record with better GOF values (due to low-frequency scaling) but with increased PGA is better than a simulation with good PGA agreement but less-than-desired frequency content match. This is especially needed in ground response analysis where frequency content can greatly affect the output and resonance effects are crucial. For this reason, along with the improvement in other earthquake characteristics, we can say that low-frequency scaling makes for better simulations for use in processes where whole earthquake records are used – such as ground response analysis.

It must also be noted that a user can use both outputs of SFFM with and without low-frequency scaling by combining the outputs from two (or more simulations) and enveloping the combined response spectra from the simulations.

The CAP may also be used to study the similarity of accelerograms as well. This provides an easier visualization of the increase of motion experienced by a site over time.

As highlighted, the simulations with and without low-frequency scaling have their advantages and fit certain demands or analyses method. While the use of low-frequency scaling

seems to be better overall as it approximates more earthquake characteristics in both the time and frequency domain, it does so at the cost of increased PGA.

The simulation of the M_w7.2 2013 Bohol earthquake was made possible using the stochastic finite-fault model employed in EXSIM_V3 by using the physical fault model obtained from various literature. The results show that despite lacking certain literature data specific to the Philippines or Bohol, usage of data from other countries with a similar geologic setting like Taiwan and Japan is acceptable and will result in good simulations. Data like the high filter frequency, shear wave velocity, density, geometric attenuation, and a certain component of the duration function (i.e. the distance-dependent factor) are all patterned after literature based on other countries while the quality factor function and stress drop value were patterned after studies in the Philippines. It must be noted that certain parameters will have to be chosen more carefully than the others – for example, the stress drop value can be done via trial and error and further supported by values for an earthquake source of similar dimension and magnitude, in this case, we adopted a value similar to a study concerning the WVF in the Philippines. Other parameters, like the duration function, will have to be determined from a combination of literature study and trial and error. The distance-dependent part of the duration can be taken from places with similar settings; however, the minimum duration will have to be adjusted as this can be thought of as dependent on the source itself and to ensure that the simulation's shape will be comparable to the recorded earthquake.

Based on the signal match between the predicted and actual earthquake records for the test cases considered in this study, the use of SFFM with low-frequency scaling shows promise as a method for obtaining earthquake records used in site-specific ground response analyses. However, as these results are based on a single large earthquake event, it is recommended to simulate more large-scale earthquake events in the Philippines to further verify the applicability of the method employed in EXSIM_V3 and the use of certain literature values. More studies are suggested to be done as well to fully understand the nature of low-frequency scaling needed and the factors behind it. As seen in the study, the low-frequency scaling phase needs a target FAS to find the range and amplification factor needed – a study phase that cannot be done unless you have records from the fault or a study in a fault that is deemed or assumed to be similar.

VI. ACKNOWLEDGEMENTS

The authors would like to acknowledge the assistance and thank Dr. Dariush Motazedian and Dr. Stephen Crane for providing a copy of EXSIM_V3 program files and its draft manual as well as providing information about certain details of the program. The authors would like to thank the Department of Science and Technology - Philippine Institute of Volcanology and Seismology (DOST - PHIVOLCS) with the help of Dr. Leonila P. Bautista and Mr. Ishmael C. Narag for the strong motion data of the October 15, 2013, Bohol earthquake. Funding for certain areas of this study was provided by research grants from the Commission on Higher Education (CHED), Engineering Research and Development for Technology (ERDT) program under the Department of Science and Technology – Science Education Institute (DOST-SEI), and the Office of the Chancellor of the University of the Philippines Diliman through the Office

of the Vice-Chancellor for Research and Development (OVCRD) through the Thesis and Dissertation grant.

REFERENCES

[1] Department of Science and Technology-Philippine Institute of Volcanology and Seismology (DOST-PHIVOLCS). 2018. Retrieved from https://www.phivolcs.dost.gov.ph/index.php/news/2049-dost-phivolcs-to-launch-philippine-earthquake-model-atlas-for-designing-earthquake-resilient-buildings on 10 July 2020.

[2] Crane S, Motazedian D. 2014. Low-frequency scaling applied to stochastic finite-fault modelling. Journal of Seismology. 18: 109-122. Retrieved from: https://www.researchgate.net/publication/259635431_Low-frequency_scaling_applied_to_stochastic_finite-fault_modeling.

[3] Atkinson G, Boore D. 2006. Earthquake ground-motion prediction equations for Eastern North America. Bulletin of Seismological Society of America. 96(6): 2181-2205. Retrieved from: https://www.researchgate.net/publication/228690474_Earthquake_Ground-Motion_Prediction_Equations_for_Eastern_North_America.

[4] Crane S, Motazedian D. ND. A guide for using EXSIM_V3: a stochastic finite-fault modelling technique with low-frequency scaling [Draft].

[5] Crane S, Motazedian D. 2011. EXSIM_V3 [Computer Program].

[6] Kramer S. 1996. Geotechnical earthquake engineering. New Jersey: Prentice-Hall, Inc.

[7] United States Geological Survey. ND. Retrieved from: https://www.usgs.gov/natural-hazards/earthquake-hazards/science/earthquake-hazards-201-technical-qa?qt-science_center_objects=0#qt-science_center_objects on 14 June 2021.

[8] Arias A. 1970. A measure of earthquake intensity. Seismic design for nuclear power plants. Hansen, RJ, editor. Cambridge, Mass: Massachusetts Institute of Technology Press. p. 438-483.

[9] Boore D. 2003. Simulation of ground motion using the stochastic method. Pure and Applied Geophysics. 160(3): 635-676. Retrieved from: https://www.researchgate.net/publication/225569447_Simulation_of_Ground_Motion_Using_the_Stochastic_Method.

[10] Motazedian D, Atkinson G. 2005. Stochastic finite-fault modelling based on a dynamic corner frequency. Bulletin of the Seismological Society of America. 95(3): 995- 1010. Retrieved from: https://www.researchgate.net/publication/228627141_Stochastic_Finite-Fault_Modeling_Based_on_a_Dynamic_Corner_Frequency.

[11] Nakamura Y. 1989. A method for dynamic characteristics estimation of subsurface using microtremor on the Ground Surface. Quarterly Report of Railway Technical Research Institute. 30(1):25-33. Retrieved from: https://www.sdr.co.jp/papers/hv_1989.pdf

[12] Nakamura Y. 2008. On the H/V spectrum. The 14th World Conference on Earthquake Engineering; Beijing, China. Retrieved from: https://www.sdr.co.jp/eng_page/papers/14wcee/14wcee_hv.pdf

[13] Sato T, Nakamura Y, Saita J. 2004. Evaluation of the amplification characteristics of subsurface using microtremor and strong motion - the studies at Mexico City. 13th World Conference on Earthquake Engineering; Vancouver, B.C., Canada. Retrieved from: https://www.researchgate.net/publication/253630796_EVALUATION_OF_THE_AMPLIFIC

ATION_CHARACTERISTICS_OF_SUBSURFACE_USING_MICROTREMOR_AND_STRONG_MOTION_-_THE_STUDIES_AT_MEXICO_CITY

[14] Department of Science and Technology - Philippine Institute of Volcanology and Seismology (DOST-PHIVOLCS). 2013. Retrieved from: http://www.phivolcs.dost.gov.ph/html/update_SOEPD/2013_Earthquake_Bulletins/October/Moment_Tensor.pdf.

[15] Department of Science and Technology - Philippine Institute of Volcanology and Seismology (DOST-PHIVOLCS). 2013. Retrieved from: http://www.phivolcs.dost.gov.ph/html/update_SOEPD/2013_Earthquake_Bulletins/October/2013_1015_0012_B3F.html.

[16] GlobalCMT Web Page. Global CMT Catalog. Retrieved from: http://www.globalcmt.org.

[17] Lagmay A, Eco R. 2014. Brief communication: on the source characteristics and impacts of the magnitude 7.2 Bohol earthquake, Philippines. Natural Hazards and Earth System Sciences. 14(10): 2795-2801. Retrieved from: https://www.researchgate.net/publication/278395726_Brief_Communication_On_the_source_characteristics_and_impacts_of_the_magnitude_72_Bohol_earthquake_Philippines.

[18] Earthquake and Megacities Initiative (EMI). 2014. The Mw7.2 15 October 2013 Bohol, Philippines earthquake: Technical Report. Diliman, Quezon City: Earthquake and Megacities Initiative (EMI). Retrieved from: https://emi-megacities.org/wp-content/uploads/2014/10/TR-14-01.pdf

[19] Felix R, Lagmay A, Norini G, Eco R. 2014. Mapping of the Inabanga fault in Bohol, Philippines using high resolution LIDAR imagery and field mapping verification. The 5th International INQUA Meeting on Paleoseismology, Active Tectonics, and Archeoseismology; Busan, Korea. The Geological Society of Korea (GSK), Korean Institute of Geoscience and Mineral Resources (KIGAM). p. 66-69. Retrieved from: https://www.earthquakegeology.com/materials/proceedings/2014_Busan.pdf

[20] Wells D, Coppersmith K. 1994. New empirical relationships among magnitude, rupture length, rupture width, rupture area and surface displacement. Bulletin of Seismological Society of America. 84(4): 974-1002. Retrieved from: https://www.researchgate.net/publication/215755871_New_Empirical_Relationships_among_Magnitude_Rupture_Length_Rupture_Width_Rupture_Area_and_Surface_Displacement.

[21] United States Geological Survey. 2013. Retrieved from: https://earthquake.usgs.gov/earthquakes/eventpage/usb000kdb4#moment-tensor.

[22] Google. 2015. Map for October 15 2013 M7.2 Bohol Earthquake [Map data: Google Earth; Google; Data SIO, NOAA, U.S. Navy, NGA, GEBCO; Image Landsat/Copernicus; Data LDEO-Columbia, NSF, NOAA]. United States.

[23] Google. 2020. Google Earth Pro (Version 7.3.3.7786 64 bit)

[24] Association of Structural Engineers of the Philippines, Inc. 2016. National Structural Code of the Philippines 2015. 7th ed. Vol I. Quezon City: Association of Structural Engineers of the Philippines, Inc.

[25] Provincial Planning and Development Office Bohol. ND. Retrieved from: https://ppdo.bohol.gov.ph/maps/thematic-maps/geologic-map/.

[26] Bureau of Mines and Geo-sciences, Ministry of Natural Resources. 1981. Geology and mineral resource of the Philippines. 1st Edition. Vol 1. Manila, Philippines: Bureau of Mines and Geo-sciences, Ministry of Natural Resources.

[27] Siddiqqi J, Atkinson G. 2002. Ground-motion amplification at rock sites across Canada as determined from the horizontal-to-vertical component ratio. Bulletin of Seismological

Society of America. 92(2):877-884. Retrieved from: https://www.researchgate.net/publication/255620935_Ground-Motion_Amplification_at_Rock_Sites_across_Canada_as_Determined_from_the_Horizontal-to-Vertical_Component_Ratio.

[28] Tsuboi S, Saito M, Ishihara Y. 2001. Verification of horizontal-to-vertical spectral ratio technique of site response using borehole seismographs. Bulletin of the Seismological Society of America. 91(3): 499-510. Retrieved from: https://pubs.geoscienceworld.org/ssa/bssa/article-abstract/91/3/499/102866/Verification-of-Horizontal-to-Vertical-Spectral?redirectedFrom=fulltext.

[29] Department of Science and Technology - Philippine Institute of Volcanology and Seismology (DOST - PHIVOLCS). 2014. October 15 2013 Bohol Earthquake Data. Quezon City: Department of Science and Technology - Philippine Institute of Volcanology and Seismology (DOST - PHIVOLCS). Recorded 2013; Processed 2014.

[30] Sokolov V, Loh C, Wen K. 2001. Site-dependent design input ground motion estimations for the Taipei area: A probabilistic approach. Probabilistic Engineering Mechanics. 16(2):177-191. Retrieved from: https://www.sciencedirect.com/science/article/abs/pii/S0266892000000217.

[31] Ghofrani H. 2012. An investigation into earthquake ground motion characteristics in Japan with emphasis on the 2011 M9.0 Tohoku earthquake [doctoral]. Ontario, Canada: University of Western Ontario.

[32] Ghofrani H, Atkinson G, Goda K. 2013. Implications of the 2011 M9.0 Tohoku Japan earthquake for the treatment of site effects in large earthquakes. Bulletin of Earthquake Engineering. 11(1):171-203. Retrieved from: https://www.researchgate.net/publication/257523469_Implications_of_the_2011_M90_Tohoku_Japan_earthquake_for_the_treatment_of_site_effects_in_large_earthquakes.

[33] Sokolov V, Loh C, Jean W. 2006. Strong ground motion source scaling and attenuation models for earthquakes located in different source zones in Taiwan. 4th International Conference on Earthquake Engineering; Taipei, Taiwan. Retrieved from: https://www.researchgate.net/publication/228570869_Strong_ground_motion_source_scaling_and_attenuation_models_for_earthquakes_located_in_different_source_zones_in_Taiwan

[34] Macias M, Atkinson G, Motazedian D. 2008. Ground motion attenuation, source, and site effects for the 26 September 2003 M 8.1 Tokachi-Oki Earthquake sequence. Bulletin of Seismological Society of America. 98(4): 1947-1963. Retrieved from: https://www.researchgate.net/publication/250074101_Ground-Motion_Attenuation_Source_and_Site_Effects_for_the_26_September_2003_M_81_Tokachi-Oki_Earthquake_Sequence.

[35] Archuleta R, Ji C. 2016. Moment rate scaling for earthquakes 3.3<=M<=5.3 with implications for stress drop. Geophysical Research Letters. 43(23): 12004-12011. Retrieved from: https://www.researchgate.net/publication/310471143_Moment_Rate_Scaling_for_Earthquakes_33_M_53_with_Implications_for_Stress_Drop_Moment_Rate_Scaling_for_Earthquakes.

[36] Ghofrani H, Atkinson G. 2011. Forearc versus Backarc attenuation of earthquake ground motion. Bulletin of Seismological Society of America. 101(6): 3032-3045. Retrieved from: https://www.researchgate.net/publication/257920749_Forearc_versus_Backarc_Attenuation_of_Earthquake_Ground_Motion.

[37] Kanao M, Ito K. 1992. Attenuation of Coda waves in the source area of the 1990 July 16 Luzon Earthquake Philippines. Bulletin of the Disaster Prevention Research Institute. 42(2): 31-51. Retrieved from: https://core.ac.uk/download/pdf/39254846.pdf.

[38] Liu C. 2006. Finite fault stochastic modelling of the 1999 Chi-Chi Taiwan Earthquake [masters]. Ottawa, Ontario, Canada: Carleton University.

[39] Ghofrani H, Atkinson G. 2014. Duration of 2011 Tohoku earthquake ground motions. Journal of Seismology. 18(3). Retrieved from: https://www.researchgate.net/publication/264082335_Duration_of_the_2011_Tohoku_earthquake_ground_motions.

[40] Moghaddam H, Fanaie N, Motazedian D. 2010. Estimation of stress drop for some large shallow earthquakes using stochastic point source and finite fault modelling. Scientia Iranica. 17(3): 217-235. Retrieved from: https://www.researchgate.net/publication/228809695_Estimation_of_Stress_Drop_for_Some_Large_Shallow_Earthquakes_Using_Stochastic_Point_Source_and_Finite_Fault_Modeling.

[41] Pulido N, Bautista B, Bautista L, Sakai H, Arai H, Kubo T. 2004. Seismic vulnerability evaluation of urban structures in Metro Manila - part 1: generation of strong ground motion from a scenario earthquake of the West Valley Fault. Asia Conference on Earthquake Engineering 2004; Manila, Philippines. Retrieved from: https://www.j-shis.bosai.go.jp/staff/nelson/papers/Pulido_ACEE_2004.pdf

[42] Japan International Cooperation Agency (JICA); Metropolitan Manila Development Authority (MMDA); Department of Science and Technology - Philippine Institute of Volcanology and Seismology (DOST - PHIVOLCS). 2004. Earthquake impact reduction study for Metropolitan Manila, Republic of the Philippines (MMEIRS).

[43] Boore D. 2009. Comparing stochastic point- and finite-source ground-motion simulations: SMSIM and EXSIM. Bulletin of the Seismological Society of America. 99(6): 3202-3216. Retrieved from: https://www.researchgate.net/publication/228530411_Comparing_stochastic_point-source_and_finite-source_ground-motion_simulations_SMSIM_and_EXSIM.

[44] Kristekova M, Kristek J, Moczo P. 2009. Time-frequency misfit and goodness-of-fit criteria for quantitative comparison of time signals. Geophysical Journal International (Internet). 178(2): 813-825. Retrieved from: https://www.researchgate.net/publication/234080676_Time-frequency_misfit_and_goodness-of-fit_criteria_for_quantitative_comparison_of_time_signals.

[45] Kristekova M, Kristek J, Moczo P, Day S. 2006. Misfit criteria for quantitative comparison of seismograms. Bulletin of the Seismological Society of America. 96(5): 1836-1850. Retrieved from: https://www.researchgate.net/publication/234080658_Misfit_Criteria_for_Quantitative_Comparison_of_Seismograms.

[46] Anderson J. 2004. Quantitative measure of the goodness-of-fit of synthetic seismograms. 13th World Conference on Earthquake Engineering; Vancouver, B.C., Canada. Retrieved from: https://www.researchgate.net/publication/267256067_Quantitative_measure_of_the_goodness-of-fit_of_synthetic_seismograms.

[47] NuQuake Computer Codes. ND. Retrieved from: http://www.nuquake.eu/Computer_Codes/index.html on 25 June 2020.

[48] Seed H, Tokimatsu K, Harder L, Chung R. 1985. Influence of SPT procedures in soil liquefaction resistance evaluations. Journal of Geotechnical Engineering. 111(12): 1425-1445.

Retrieved from: https://ascelibrary.org/doi/pdf/10.1061/%28ASCE%290733-9410%281985%29111%3A12%281425%29.

[49] Seed R, Cetin K, Moss R, Kammerer A, Wu J, Pestana J, Riemer M, Sancio R, Bray J, Kayen R, Faris A. 2003. Recent advances in soil liquefaction engineering: a unified and consistent framework. 26th Annual ASCE Los Angeles Geotechnical Spring Seminar (Keynote Presentation), Long Beach California: Earthquake Engineering Research Center, College of Engineering, University of California, Berkeley. Report No EERC 2003-06. Retrieved from: https://www.researchgate.net/publication/314359545_C14_Recent_advances_in_soil_liquefaction_engineering_A_unified_and_consistent_framework